Article

Journal of
Nanoscience and Nanotechnology
Vol. 20, 197–205, 2020
www.aspbs.com/jnn

Effects of Plasma Treatment on the Composition and Phase Changes of Sputter-Deposited SnO_x Thin Films

Han Byeol Seo[1], Byung Seong Bae[2], Hyo In Bang[3], and Eui-Jung Yun[3,*]

[1] Department of NanoBio Tronics, Hoseo University, Asan, Chungnam 31499, Republic of Korea
[2] Department of Display Engineering, Hoseo University, Asan, Chungnam 31499, Republic of Korea
[3] Department of ICT Automotive Engineering, Hoseo University, Dangjin, Chungnam 31702, Republic of Korea

This study examined the effects of the plasma treatment of CF_4 or SF_6 on the properties of tin oxide (SnO_x) thin films prepared at room temperature using a radio frequency sputtering technique. The properties of the samples were characterized by dynamic-secondary ion mass spectrometry, X-ray photoelectron spectroscopy (XPS), X-ray diffraction (XRD), and Hall Effect measurements. All untreated samples showed Sn^{4+} and Sn^{2+} XPS peak area percentages of 57.6 and 34.6%, respectively, indicating a larger amount of SnO_2 phase in the samples than SnO. The samples treated with CF_4 plasma exhibited the maximum and minimum Sn^{4+} and Sn^{2+} peak areas, respectively, at a treatment time of 35 s. This was attributed to the maximum oxygen atomic percentage at 35 s and the injection of additional carbon and fluorine into the sample with increasing treatment time. On the other hand, in the case of samples treated with SF_6 plasma, the Sn^{4+} peak area increased with increasing treatment time while the Sn^{2+} peak area decreased. This suggests that SnO_2 is a stronger phase for samples treated with SF_6 plasma for a longer duration. Furthermore, the changes in the Sn^{4+} and Sn^{2+} peak areas of the samples treated with CF_4 plasma were much larger than those of the samples treated with SF_6 plasma, which indicates that CF_4 plasma has a larger impact on the properties of the samples. This difference in impact showed a correlation with the sharper decrease in the number of oxygen vacancies for CF_4 plasma-treated samples. These results were attributed to the introduction of additional fluorine and carbon into CF_4 plasma-treated samples compared to the SF_6 plasma-treated ones. In addition, XRD showed that the plasma treatment did not affect the amorphous phase in the samples.

Keywords: Plasma Treatment, Tin-Oxide (SnO), SF_6 Ambient, CF_4 Ambient.

1. INTRODUCTION

Complementary metal–oxide–semiconductor (CMOS) devices have attracted considerable attention as an alternative approach to realizing radio frequency (RF) identification (ID) tags or drivers for the next-generation display applications. On the other hand, they require both *n*-type and *p*-type thin film transistors (TFTs) with high performance [1–10]. Recently, tin oxide (SnO_x) thin-films have become good candidates for the development of high performance CMOS circuits because tin dioxide (SnO_2) and tin monoxide (SnO) thin films can be used for *n*-type and *p*-type channel layers in the fabrication of high-performance TFTs, respectively [1, 11–18].

Recently, it was reported that a fluorine (F) plasma treatment of a *p*-type SnO active layer that was formed by physical vapor deposition and post-annealed at 200 °C could reduce the surface roughness of the crystallized SnO active layer and passivate the oxygen vacancies (V_O) and interface traps, resulting in high performance *p*-type SnO TFT devices [8]. Furthermore, the plasma treatment of amorphous indium gallium zinc oxide (a-IGZO) with fluorine or sulfur ambient gas played a positive role in the electrical properties of a-IGZO thin films and the stability of a-IGZO TFTs [19, 20]. On the other hand, the properties of low temperature-processed SnO_x active layers need to be optimized to improve the device properties and stability of flexible SnO_x-based TFTs. Up to now, details of the properties of low temperature-processed SnO_x thin films are unclear and the device properties of flexible SnO-based

*Author to whom correspondence should be addressed.

TFTs are still far from acceptable for practical applications. Moreover, there are few reports on the effects of the plasma treatment on the properties of SnO_x thin films deposited at low temperatures (<200 °C) using a SnO sputtering target. Therefore, in this study, the effects of a plasma treatment on the properties of SnO_x thin films deposited at room temperature (RT) using a SnO sputtering target were examined systematically using CF_4 and SF_6 plasma treatments.

2. EXPERIMENTAL DETAILS

SnO_x thin films, 100 nm in thickness, were deposited on 300-nm-thick SiO_2-coated Si or glass substrates at room temperature (RT) using a SnO (99.99%, 2 inch diameter) sputtering target under the following conditions: radio frequency (RF) power of 50 W, working pressure of 0.533 Pa, and oxygen ratio of 12%. Pure argon (99.999%) and oxygen gas mixtures were used as the reaction gas and the total flow rate was 25 sccm. The substrate-to-target distance was 10 cm for all depositions. The substrate was rotated at 13 rpm to deposit the SnO_x thin films with a uniform thickness. To examine the effects of the CF_4 or SF_6 plasma treatment on the properties of the samples, the SnO_x thin films were treated with CF_4 or SF_6 plasma after deposition using reactive ion etching (RIE) equipment under the following conditions: flow rate of 20 cm^3/min, working pressure of 1.33×10^{-3} Pa, RF power of 180 W, and treatment time range of 0 to 55 s. The SnO_x thin films were annealed at 150 °C for 1 hour in air after the plasma treatment.

The contents (at. %) and chemical bonding states of Sn, O, C, F, and S in the SnO_x thin films were characterized by X-ray photoelectron spectroscopy (XPS). The changes in the depth profiles of Sn, O, C, F, S, and Si in the samples were examined by dynamic secondary ion mass spectrometry (D-SIMS). The structures and the surface morphologies of the SnO_x films were characterized by using X-ray diffraction (XRD) with a Cu $K\alpha_1$ radiation source ($\lambda = 0.15406$ nm) and field-emission scanning electron microscopy (FE-SEM), respectively. The electrical properties of the SnO_x thin films were measured at RT using a Hall Effect measurement system according to the van der Pauw configuration after forming Ohmic contacts with a 100-nm-thick Al layer using a sputtering system, followed by alloying at 150 °C in air for 1 hour.

3. RESULTS AND DISCUSSION

Figure 1 presents the selected D-SIMS depth profiles, which exhibit typical intensity variations in Sn, O, C, F, S, and Si concentrations in the SnO_x/SiO_2 bi-layer structures treated with two different plasmas, CF_4 or SF_6, for 0–55 s. Figure 1(a) shows that meaningful amounts of F and S were observed even in the untreated samples. As shown in Figures 1(b) and (c), in the case of the samples treated with CF_4 plasma, the CF_4 plasma treatment caused the diffusion of F into the sample surface at a much higher concentration than C and resulted in the introduction of a noticeable amount of C at a long plasma treatment time of 55 s. For the samples treated with SF_6 plasma, a large amount of F also diffused into the SnO_x surface. The SF_6 plasma treatment, however, did not result in the injection of S into the SnO_x films, as evident in Figures 1(d) and (e). F was reported to either reduce V_O or generate F-related donor defects in the samples, which results in a decrease or increase in resistivity, respectively [8, 19, 20]. The Hall measurement results showed that the samples untreated and treated with CF_4 or SF_6 plasmas exhibited the insulating behavior. This suggests that regardless of the plasma treatment, the high resistance of the samples is related to the introduction of F into the samples. Note that the Sn in SnO_x films can react with F, resulting in a decrease in the number of V_O donor defects, which causes a decrease in the electron concentration and an increase in resistance. Furthermore, Figure 1 shows that the composition of the samples treated with CF_4 and SF_6 plasma was close to the *n*-type tin dioxide (SnO_2).

To visualize the changes in the SIMS depth profiles of F, C, and S more effectively, the percentage variations in the F, C, and S concentrations in the samples treated with CF_4 and SF_6 plasmas were replotted using the data in Figure 1 and are shown in Figure 2. The concentration changes were normalized to the initial concentrations in the untreated sample using Eq. (1):

$$\Delta I(\%) = \frac{I_{\text{treated}} - I_{\text{untreated}}}{I_{\text{untreated}}} \times 100 \quad (1)$$

where $I_{\text{untreated}}$ and I_{treated} are the concentrations of F, C, and S in the samples untreated and treated with two plasmas (CF_4 or SF_6), respectively. In Eq. (1), a negative (positive) value of ΔI means a decrease (increase) of the concentrations of F, C, and S in the sample treated with the plasmas compared to the initial concentration in the untreated sample. In the case of the samples treated with CF_4 plasma, as shown in Figure 2(a), CF_4-treated samples for a long treatment time of 55 s showed very large increases in the C concentration in the SnO_x films, whereas those CF_4-treated at 35 and 45 s exhibited lower C concentrations inside the samples. These suggest that a large amount of C diffused into the samples during the treatment for a longer time of 55 s, whereas some C diffused out to the ambient during the treatment at shorter times of 35 and 45 s. As plotted in Figure 2(b), however, a much larger amount F was observed at the film surface and a meaningful amount of F was detected inside all the CF_4-treated films. This F concentration inside the CF_4-treated films increased at 35 s and decreased slightly with increasing the plasma treatment time from 35 to 55 s, suggesting that F diffusion from the ambient into the films was maximized at 35 s.

On the other hand, in the case of the samples treated with SF_6 plasma, the S concentration at the narrow surface

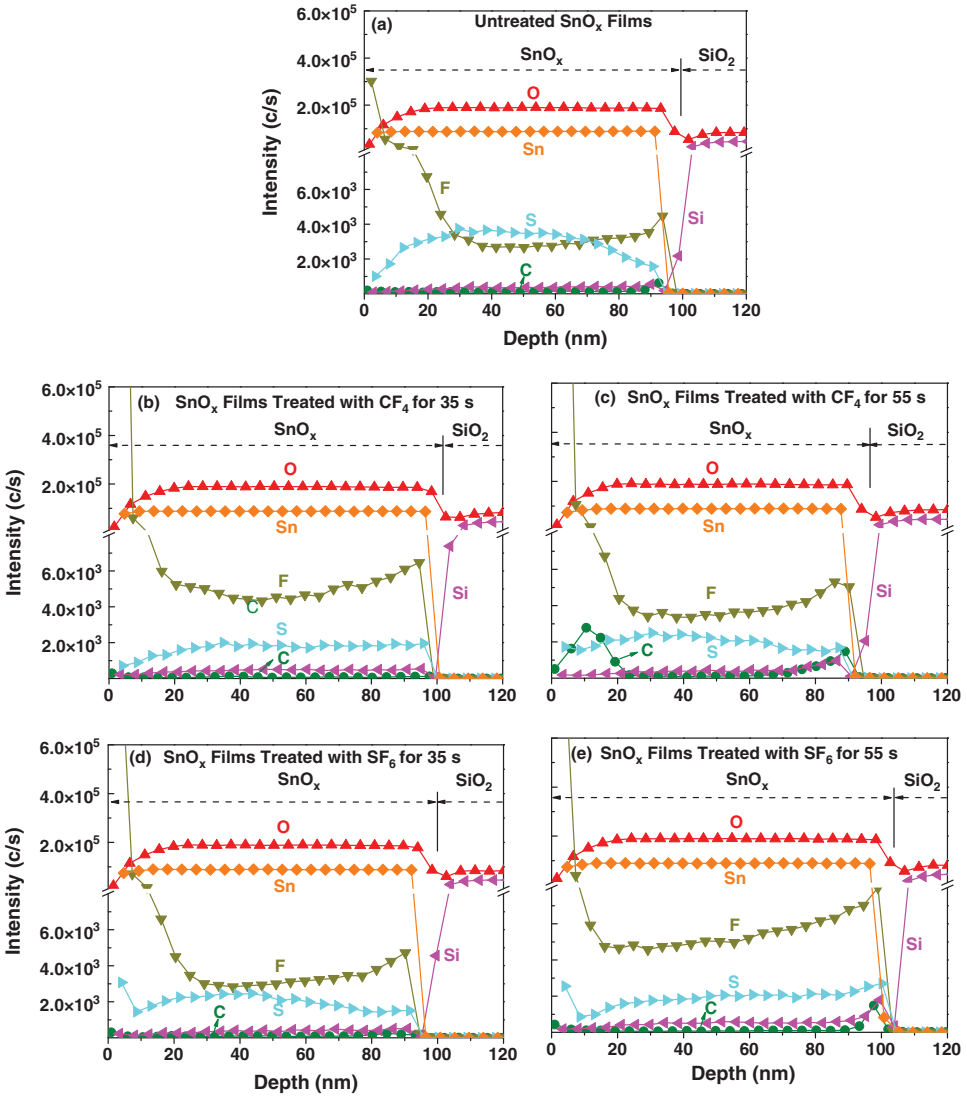

Figure 1. Intensity variations in the tin (Sn), oxygen (O), carbon (C), fluorine (F), sulfur (S), and silicon (Si) concentrations in the SnO_x/SiO_2 bi-layer structures (a) untreated, treated with CF_4 plasma for (b) 35 and (c) 55 s, and treated with SF_6 plasma for (d) 35 and (e) 55 s, which were obtained from the SIMS depth profiles.

(<10 nm) of the SnO_x films increased steeply, whereas that inside the films decreased, as shown in Figure 2(c), suggesting that a noticeable amount of S diffused out to the film surface during the SF_6 plasma treatment. Moreover, the F depth profiles in Figure 2(d) showed that the F concentration in the SnO_x films increased with increasing SF_6 plasma treatment time, indicating that a large amount of F diffused into the films during treatment. The increased F and C concentrations in the films can cause a decrease in the number of V_O in the plasma-treated films as a result of the occupation of V_O sites by the increased F and C.

Figure 3 shows XRD patterns of SnO_x films untreated and treated with CF_4 or SF_6 plasma at different treatment times, 0–55 s, indicating that the prepared films have a very fine nanocrystalline or amorphous phase. This is because at room substrate temperature, the adatom mobility and reactions among Sn, O, C, S, and F are restricted on the substrate surface, resulting in a large number of defects in the SnO_x films untreated and treated with CF_4 or SF_6 plasmas. Therefore, very fine nanocrystalline or amorphous films are formed. As shown in Figure 3, regardless of the plasma treatment, all samples revealed two halo peaks centered at ~31.4° and ~54.8° 2θ, corresponding to the (101) and (220) orientations of nanocrystalline SnO_2, respectively [2, 15, 16, 21, 22]. This suggests that the samples untreated and treated with CF_4 and SF_6 plasmas are mainly the *n*-type SnO_2 phase, as confirmed by the SIMS

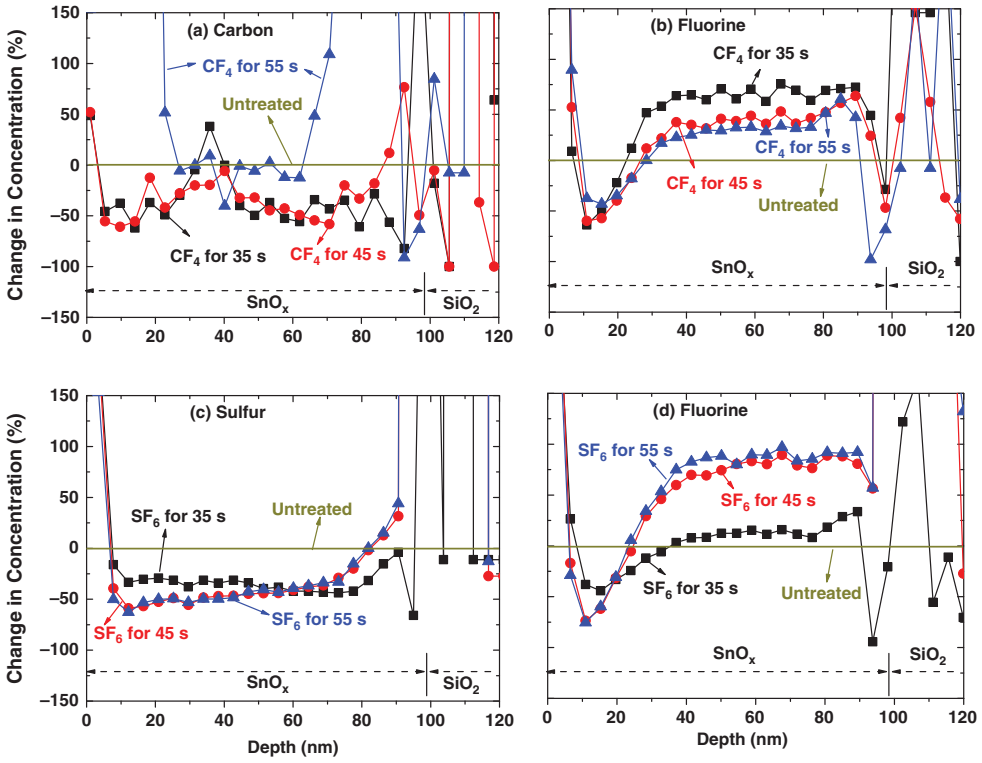

Figure 2. Percentage variations in (a) carbon (C) and (b) fluorine (F) concentrations in the SnO_x/SiO_2 bi-layer structures treated with CF_4 plasma, and percentage changes in (c) sulfur (S) and (d) F concentrations in the samples treated with SF_6 plasma, which were obtained from the SIMS depth profiles shown in Figure 1. The concentrations were normalized to those in the untreated sample; the lines are a guide for the eye.

result. Therefore, the plasma treatment did not affect amorphous phase in the sample.

The carbon (C) 1*s* reference peak at 284.6 eV was used to calibrate all binding energies measured by XPS. Two Sn 3*d* narrow-scan XPS peaks for the SnO_x thin films, which were observed at binding energies of 486.3 and 494.7 eV, were associated with the spin orbit of Sn $3d_{5/2}$ and Sn $3d_{3/2}$, respectively [2, 8, 9, 15, 16, 18, 21, 23]. The Sn $3d_{5/2}$ narrow-scan XPS spectra of the SnO_x films prepared in this study were fitted using three Gaussian peaks (GPs) related to the Sn^0, Sn^{2+}, and Sn^{4+} peaks centered at approximately 485–485.6, 486.2–486.8, and 486.9–487.6 eV, respectively, which correspond to metallic Sn, *p*-type SnO, and *n*-type SnO_2.

Figures 4(a) and (b) present selected examples of the Sn $3d_{5/2}$ narrow-scan XPS spectra fitted using three GPs in the samples untreated and treated with CF_4 plasma for 55 s, respectively. The fitting of the Sn $3d_{5/2}$ peaks using three GPs was excellent. As plotted in Figure 4(a), for the SnO_x films untreated with the plasma, the percentage areas of the Sn^0 peaks centered at 485.23 eV, Sn^{2+} peaks at 486.2 eV, and Sn^{4+} peaks at 486.72 eV were 7.8, 34.6, and 57.6%, respectively. Figure 4(b) also shows that the percentage areas of the Sn^0 peaks centered at 485.19 eV, Sn^{2+} peaks at 486.22 eV, and Sn^{4+} peaks at 486.73 eV were 5.2, 37.1, and 57.7%, respectively, for the SnO_x films treated with the CF_4 plasma for 55 s.

Figure 5 shows the percentage areas of the three GPs as a function of the plasma treatment time for the samples untreated and treated with CF_4 or SF_6 plasma, which were extracted after fitting the Sn $3d_{5/2}$ peaks using the three Sn^0, Sn^{2+}, and Sn^{4+} GPs, as shown in Figure 4. As plotted in Figure 5, for the untreated samples (plasma treatment time = 0 s), the Sn^{4+} and Sn^{2+} XPS peak area percentages were 57.6 and 34.6%, respectively. This suggests that there is a larger amount of SnO_2 phase than that SnO in the untreated sample. This result is in good agreement with the SIMS result shown in Figure 1. In the case of the samples treated with CF_4 plasma, as shown in Figure 5(a), the Sn^{4+} and Sn^{2+} peak area percentages increased and decreased, respectively, with increasing treatment time to 35 s, which was related to an increase in the concentration of Sn^{4+} ions due to the introduction of more O and F by the CF_4 plasma treatment. This is in agreement with recent reports showing that an increase in the amount of O within the SnO_x films results in an increase in the concentration of Sn^{4+} ions [24]. Furthermore, according to the XPS reference page [25], the Sn^{4+} ions can also be increased if the increased F generates SnF_4. As the treatment time of CF_4 plasma was increased to more than 35 s, the Sn^{4+}

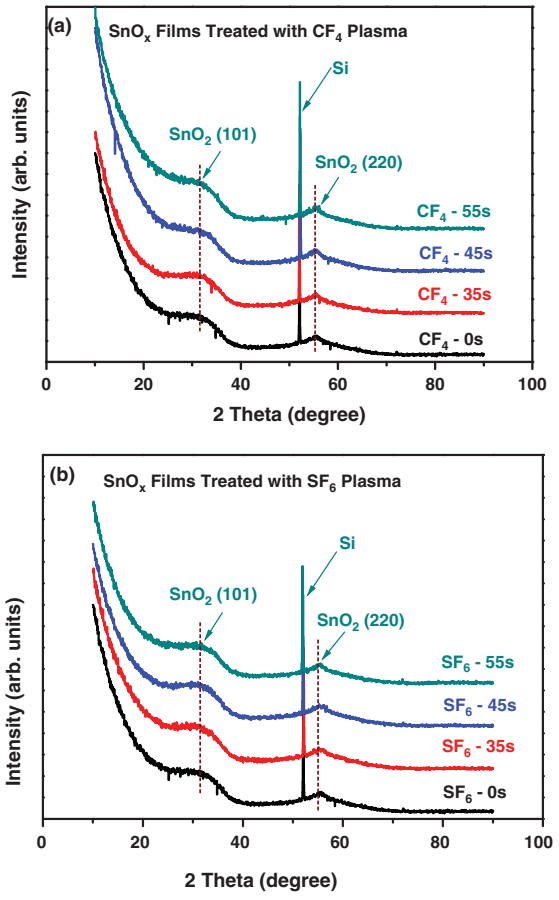

Figure 3. X-ray diffraction (XRD) patterns of SnO_x films that were treated with (a) CF_4 and (b) SF_6 plasma for various treatment times.

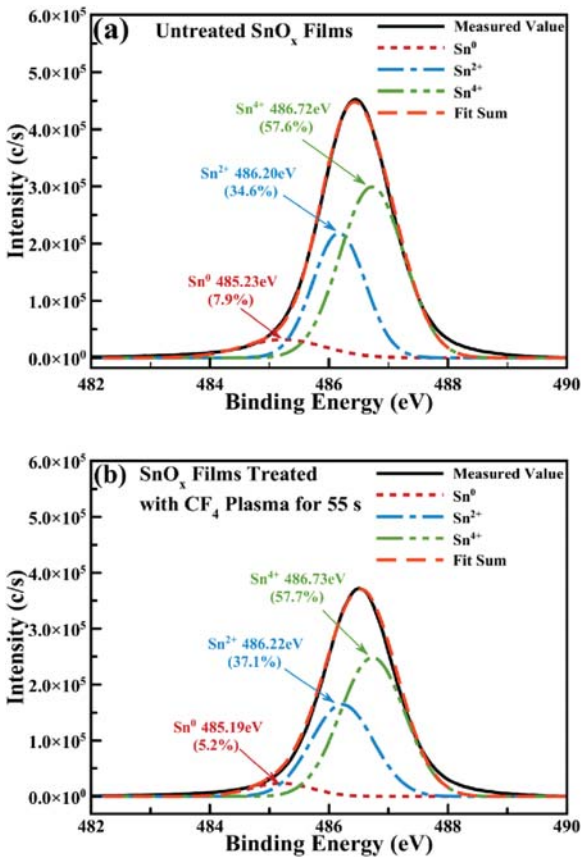

Figure 4. Selected Sn $3d_{5/2}$ narrow-scan XPS spectra fitted using three Gaussian peaks (GPs) for the SnO_x films (a) untreated and (b) treated with CF_4 plasma for a long treatment time of 55 s.

peak area percentage decreased, whereas the Sn^{2+} peak area percentage increased, which was associated with a decrease in the amount of Sn^{4+} ions and an increase in the amount of Sn^{2+} ions in the samples, respectively, due to the reduction of O and F incorporation and the introduction of more C, as confirmed by Figures 2(a) and (b).

On the other hand, for the samples treated with SF_6 plasma, the Sn^{4+} peak area percentage increased slightly, whereas the Sn^{2+} peak area percentage decreased monotonically with increasing treatment time from 0 to 55 s, as shown in Figure 5(b). These were attributed to an increase in the amount of Sn^{4+} ions and a decrease in the amount of Sn^{2+} ions in the samples, respectively, due to the increased level of O and F incorporation and the decrease in S concentration inside the SF_6-treated samples with increasing plasma treatment time, as confirmed by Figures 2(c) and (d). Here, the increased F causes an increase in the amount of Sn^{4+} ions in the samples treated with SF_6 plasma by producing SnF_4, whereas the decreased S causes a decrease in the amount of Sn^{2+} ions by the reduction of SnS formation [25].

The O 1*s* narrow-scan XPS spectra of the SnO_x films untreated and treated with CF_4 and SF_6 plasmas at various treatment times were also fitted using three GPs related to the low, middle, and high peaks (LP, MP, and HP) centered at 529.8–530.1, 531–531.1, and 531.6–531.9 eV, respectively. The LP was attributed to O^{2-} ions surrounded by Sn and O metal atoms in a fully oxidized stoichiometric SnO_x system. The MP was also assigned to O^{2-} ions in the oxygen-deficient regions within the SnO_x matrix and was associated with V_O defects, whereas HP was correlated with chemisorbed or dissociated oxygen or to O–H bonding near the film surface [26–29].

Figures 6(a) and (b) show selected examples of the O 1*s* narrow-scan XPS spectra fitted using the LP, MP, and HP GPs in the samples untreated and treated with CF_4 plasma for 55 s, respectively. As shown in Figure 6(a), for the untreated SnO_x films, the percentage areas of LP centered at 530.1 eV, MP at 531 eV, and HP at 531.8 eV were 49.7, 38, and 12.3%, respectively. On the other hand, Figure 6(b) shows that the percentage areas of LP centered at approximately 530.1 eV, MP at 531 eV, and HP at 531.5 eV were 62.6, 21.4, and 16%, respectively, for the

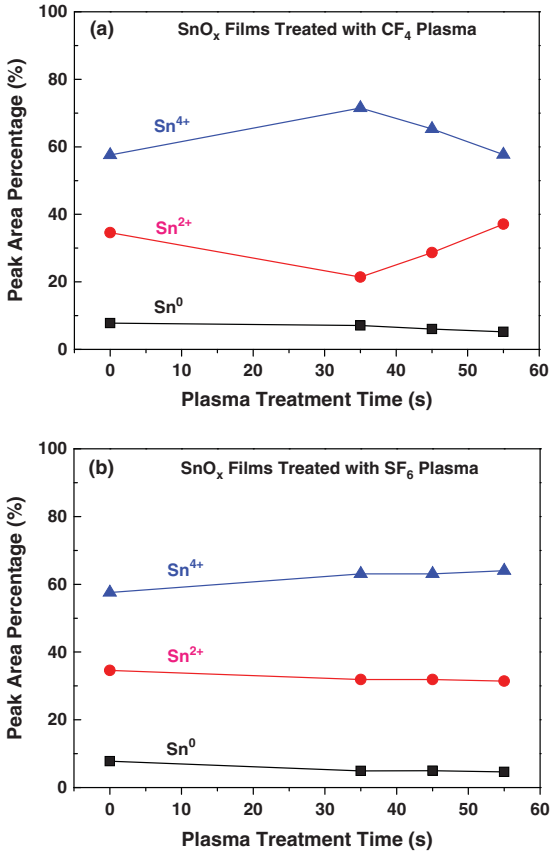

Figure 5. Peak area percentage characteristics of three Gaussian peaks (GPs) as a function of the plasma treatment time obtained from the Sn $3d_{5/2}$ narrow scan XP spectra of SnO_x films treated with (a) CF_4 and (b) SF_6 plasmas. These results were obtained after fitting the $3d_{5/2}$ peaks using the three Sn^0, Sn^{2+}, and Sn^{4+} GPs, as shown in Figure 4.

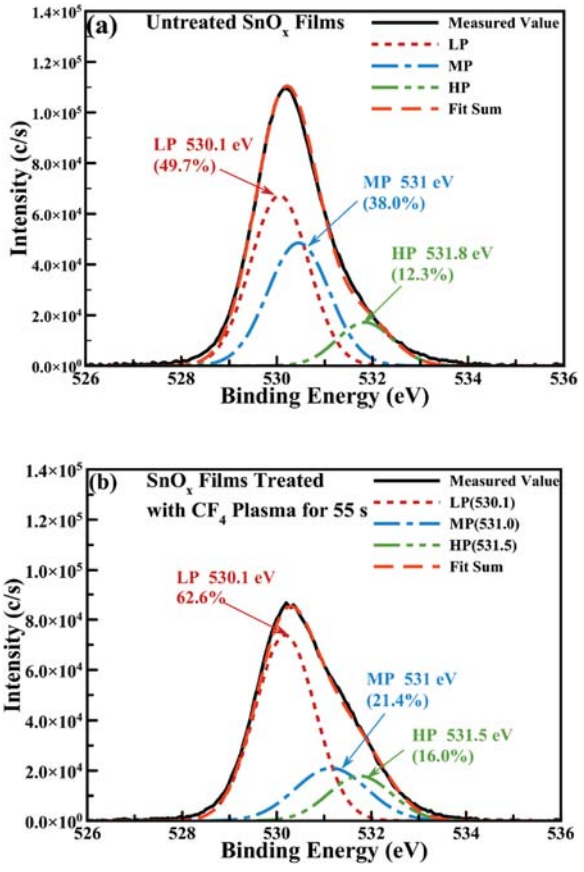

Figure 6. Selected O 1*s* narrow-scan XPS spectra fitted using three low peak (LP), middle peak (MP), and high peak (HP) Gaussian peaks for the SnO_x films (a) untreated and (b) treated with CF_4 plasma for a long treatment time of 55 s.

SnO_x films treated with CF_4 plasma for a treatment time of 55 s.

Figure 7 also shows the percentage areas of the three GPs as a function of the plasma treatment time for the samples treated with CF_4 or SF_6 plasma, which were obtained after fitting the O 1*s* peaks using the three LP, MP, and HP GPs, as shown in Figure 6. In the case of the samples treated with CF_4 plasma, with increasing treatment time to 35 s, the LP and MP areas increased and decreased considerably, respectively, which indicates that the in-diffusion of O and F in the sample surface was enhanced during the plasma treatment, as shown in Figures 2(b) and 5(a). The introduction of F and O into the samples causes a reaction of Sn–F and Sn–O, resulting in a decrease in the number of V_O donor defects [8, 19], which results in a decrease in the percentage areas of MP. On the other hand, as shown in Figure 7(a), for the samples treated with CF_4 plasma at a longer treatment time of 45 s, the decrease in MP and increase in LP were retarded. The retardation of the decrease in MP area can be explained by the following argument. When the SnO_x films were treated with CF_4 plasma for a longer treatment time of 45 s, the in-diffusion of F from the chamber into the film reduced, as evident in Figure 2(b), resulting in a decrease in the number of V_O, which impedes the decrease in MP area. In contrast, the samples treated with CF_4 plasma for 55 s exhibited an enhancement of the decrease in MP area. This was also related mainly to the enhanced reaction of Sn metal with C and F due to in-diffused C and F, as confirmed by Figures 2(a) and (b), giving rise to an acceleration of the decrease in the number of V_O.

Compared to those treated with CF_4 plasma for the same time, the samples treated with SF_6 plasma for a treatment time of 35 s showed a smaller decrease in MP and a smaller increase in LP areas because smaller amounts of O and F were diffused into the sample surface during plasma treatment, as shown in Figures 2(d) and 7(b). With increasing SF_6 plasma treatment time to 45 s, however, the decrease in MP and increase in LP were enhanced owing to the accelerated in-diffusion of F from the chamber into the film, as shown in Figure 2(d). With further increases

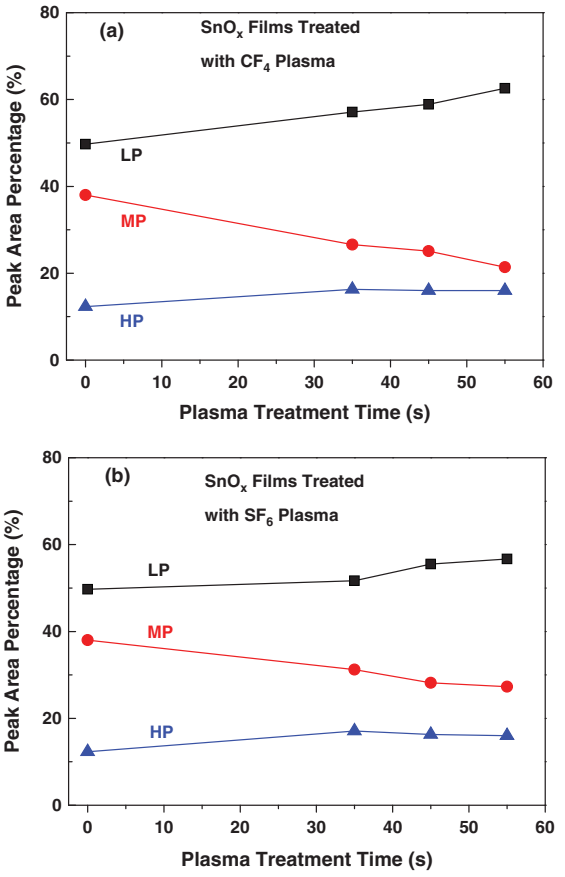

Figure 7. Peak area percentage characteristics of three Gaussian peaks (GPs) as a function of the plasma treatment time obtained from the O 1*s* narrow scan XPS spectra of SnO_x films treated with (a) CF_4 and (b) SF_6 plasmas. These results were obtained after fitting the O 1*s* peaks using the low peak (LP), middle peak (MP), and high peak (HP) GPs, as shown in Figure 6.

in plasma treatment time to 55 s, the decrease in MP area slowed, as shown in Figure 7(b), which was attributed to the retarded in-diffusion of F to the films, as confirmed by Figure 2(d).

Based on the result shown in Figure 5, the changes in Sn^{4+} and Sn^{2+} peak areas for the samples treated with CF_4 plasma were much larger than those treated with SF_6 plasma, indicating that CF_4 plasma has a larger impact on the properties of the samples. This difference in impact shows a correlation with the sharper decrease in the number of oxygen vacancies for the CF_4 plasma-treated samples, as confirmed by Figure 7. Figure 7 also showed that the HP areas were increased after the samples are treated with CF_4 or SF_6 plasma, suggesting that a larger amount of O or H appears near the surfaces of the plasma-treated SnO_x films.

The full width at half maximum (FWHM) value of the deconvoluted MP components for the samples untreated with two plasmas was 1.52 eV. The FWHM values of those for the samples treated with CF_4 plasma for 35, 45, and 55 s were determined from XPS results to be 1.64, 1.83, and 1.85 eV, respectively. On the other hand, those for the samples treated with SF_6 plasma for 35, 45, and 55 s were 1.58, 1.55, and 1.70 eV, respectively. These results suggest that the increase in the FWHM of MP occurred in all samples treated with two plasmas, and that the increase in FWHM for the samples treated with CF_4 plasma was larger than that for the samples treated with SF_6 plasma. This confirmed that CF_4 plasma had a larger impact on the properties of the samples than SF_6 plasma. We believe that the increase in the FWHM of MP in the samples treated with plasmas is mainly due to the changes in the binding energy distribution of O^{2-} ions in the oxygen-deficient regions within the SnO_x matrix resulting from the plasma treatments.

Figure 8 shows the FE-SEM top images of SnO_x films untreated and treated with CF_4 and SF_6 plasmas as a function of the treatment time. As can be seen, plasma-treated films had smoother surface morphologies. We can suggest that the smoother morphologies in the SnO_x films treated with plasmas are due to the surface etching effect that occurred as a result of plasma treatment. However, the plasma treatment did not cause the increased grain sizes inside the films treated with plasmas because the SnO_x films had an amorphous structure, regardless of plasma treatment, as is evident in Figure 3.

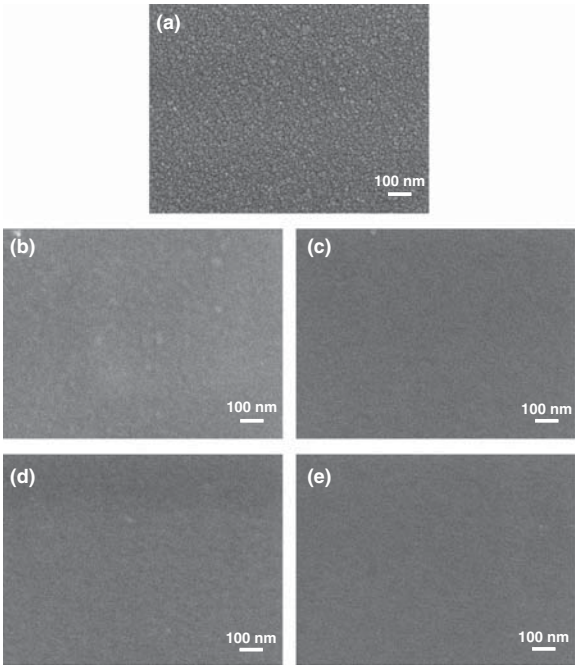

Figure 8. FE-SEM top images of the SnO_x films (a) untreated, treated with CF_4 plasma for (b) 35 and (c) 55 s, and treated with SF_6 plasma for (d) 35 and (e) 55 s.

4. CONCLUSION

This study examined the effects of CF_4 and SF_6 plasma treatments on the properties of SnO_x thin films deposited at room temperature using a SnO sputtering target. In the case of the samples treated with CF_4 plasma, the introduction of a large amount of F by the CF_4 plasma treatment at 35 s caused a significant increase in the SnO_2 phase and a considerable decrease in SnO phase in the samples. As the treatment time of CF_4 plasma was increased to more than 35 s, the incorporated F was reduced and a noticeable amount of C was introduced, resulting in a decrease in SnO_2 phase and an increase in SnO phase in the samples. The introduction of F, C, and O into the samples also produced a meaningful decrease in the number of oxygen vacancies in the CF_4-treated samples due to a reaction of Sn with F, C, and O, which was confirmed by a decrease in the MP area. On the other hand, for the samples treated with SF_6 plasma, the Sn^{4+} ions increased slightly whereas the Sn^{2+} ions decreased monotonically because of the increase in F concentration and the decrease in S concentration inside the plasma-treated samples with increasing the plasma treatment time. Moreover, the increase in F and O inside the SF_6 plasma-treated samples caused a monotonic decrease in number of oxygen vacancies in the samples. The changes in the Sn^{4+}, Sn^{2+}, MP, and LP peak areas for the samples treated with CF_4 plasma were much larger than those of the samples treated with SF_6 plasma, indicating that CF_4 plasma has a larger impact on the properties of samples. This stronger impact shows a correlation with the sharper decrease in the number of oxygen vacancies for CF_4 plasma-treated samples. All samples prepared in this study had mainly amorphous phases with some broad peaks of nanocrystalline *n*-type SnO_2 and the plasma treatment did not affect the structural properties of the samples.

Acknowledgments: This study was supported by the Basic Science Research Program through the National Research Foundation of Korea (NRF) funded by the Ministry of Education (NRF-2016R1D1A3B03932570).

References and Notes

1. Fortunato, E., Barquinha, P. and Martins, R., **2012**. Oxide semiconductor thin-film transistors: A review of recent advances. *Advanced Materials*, *24*(22), pp.2945–2986.
2. Guo, L., Zhao, M., Zhuang, D., Gong, Q., Tan, H., Cao, M. and Ouyang, L., **2016**. A study on phase transformation of SnO_x thin films prepared by reactive magnetron sputtering. *Materials Science in Semiconductor Processing*, *46*, pp.35–38.
3. Qiang, L., Liu, W., Pei, Y., Wang, G. and Yao, R., **2017**. Trap states extraction of *p*-channel SnO thin-film transistors based on percolation and multiple trapping carrier conductions. *Solid-State Electronics*, *129*, pp.163–167.
4. Martins, R., Nathan, A., Barros, R., Pereira, L., Barquinha, P., Correia, N., Costa, R., Ahnood, A., Ferreira, I. and Fortunato, E., **2011**. Complementary metal oxide semiconductor technology with and on paper. *Advanced Materials*, *23*(39), pp.4491–4496.
5. Ju, C., Park, C., Yang, H., Kim, U., Kim, Y.M. and Char, K., **2016**. High mobility field effect transistor of SnO_x on glass using HfO_x gate oxide. *Current Applied Physics*, *16*(3), pp.300–304.
6. Lee, J.-H., Choi, Y.-J., Jeong, C.-Y., Jung, D.-K., Ham, S. and Kwon, H.-I., **2016**. Electrical instability of *p*-channel SnO thin-film transistors under light illumination. *IEEE Electron Device Letters*, *37*(3), pp.295–298.
7. Azmi, A., Lee, J., Gim, T.J., Choi, R. and Jeong, J.K., **2017**. Performance improvement of *p*-channel tin monoxide transistors with a solution-processed zirconium oxide gate dielectric. *IEEE Electron Device Letters*, *38*(11), pp.1543–1546.
8. Chen, P.-C., Chiu, Y.-C., Zheng, Z.-W., Cheng, C.-H. and Wu, Y.-H., **2017**. Influence of plasma fluorination on *p*-type channel tin-oxide thin film transistors. *Journal of Alloys and Compounds*, *707*, pp.162–166.
9. Luo, H., Liang, L. and Cao, H., **2017**. Carrier trapping anisotropy in ambipolar SnO thin-film transistors. *Solid-State Electronics*, *129*, pp.88–92.
10. Ahn, J.S., Pode, R. and Lee, K.B., **2016**. Study of Cu-doped SnO thin films prepared by reactive co-sputtering with facing targets of Sn and Cu. *Thin Solid Films*, *608*, pp.102–106.
11. Ogo, Y., Hiramatsu, H., Nomura, K., Yanagi, H., Kamiya, T., Hirano, M. and Hosono, H., **2008**. P-channel thin-film transistor using *p*-type oxide semiconductor, SnO. *Applied Physics Letters*, *93*(3), pp.032113-1–032113-3.
12. Liang, L.Y., Liu, Z.M., Cao, H.T., Yu, Z., Shi, Y.Y., Chen, A.H., Zhang, H.Z., Fang, Y.Q. and Sun, X.L., **2010**. Phase and optical characterizations of annealed SnO thin films and their *p*-type TFT application. *Journal of the Electrochemical Society*, *157*(6), pp.H598–H602.
13. Hsu, P.C., Chen, W.C., Tsai, Y.T., Kung, Y.C., Chang, C.H., Hsu, C.J., Wu, C.C. and Hsieh, H.H., **2013**. Fabrication of *p*-type SnO thin-film transistors by sputtering with practical metal electrodes. *Japanese Journal of Applied Physics*, *52*(5S1), pp.05DC07-1–05DC07-6.
14. Hsu, P.C., Chen, W.C., Tsai, Y.T., Kung, Y.C., Chang, C.H., Wu, C.C. and Hsieh, H.H., **2014**. Sputtering deposition of *p*-type SnO films using robust Sn/SnO_2 mixed target. *Thin Solid Films*, *555*, pp.57–61.
15. Lin, S.-S., Tsai, Y.-S. and Bai, K.-R., **2016**. Structural and physical properties of tin oxide thin films for optoelectronic applications. *Applied Surface Science*, *380*, pp.203–209.
16. Lin, S.-S., Fan, S.-Y. and Tsai, Y.-S., **2017**. Effects of annealing on wettability and physical properties of SnO thin films deposited at low RF power densities. *Ceramics International*, *43*(2), pp.1802–1808.
17. Kim, H.-J., Jeong, C.-Y., Bae, S.-D., Lee, J.-H. and Kwon, H.-I., **2017**. Charge transport mechanism in *p*-channel tin monoxide thin-film transistors. *IEEE Electron Device Letters*, *38*(4), pp.473–476.
18. Nguyen, A. H.-T., Nguyen, M.-C., Choi, J., Han, S., Kim, J. and Choi, R., **2017**. Electrical performance enhancement of *p*-type tin oxide channel thin film transistor using aluminum doping. *Thin Solid Films*, *641*, pp.24–27.
19. Furuta, M., Jiang, J., Hung, M.P., Toda, T., Wang, D. and Tatsuoka, G., **2016**. Suppression of negative gate bias and illumination stress degradation by fluorine-passivated In–Ga–Zn–O thin-film transistors. *ECS Journal of Solid State Science Technology*, *5*(3), pp.Q88–Q91.
20. Choi, J., Bae, B.S. and Yun, E.-J., **2018**. Effects of SF_6 plasma treatment on the properties of InGaZnO thin films. *Japanese Journal of Applied Physics*, *57*(3S1), pp.03DA01-1–03DA01-6.
21. Yang, J., Pi, S., Han, Y., Fu, R., Meng, T. and Zhang, Q., **2016**. Characteristic of bismuth-doped tin oxide thin-film transistors. *IEEE Transactions on Electron Devices*, *63*(5), pp.1904–1909.
22. Zhu, B.L., Zhao, X., Hu, W.C., Li, T.T., Wu, J., Gan, Z.H., Liu, J., Zeng, D.W. and Xie, C.S., **2017**. Structural, electrical,

and optical properties of F-doped SnO or SnO_2 films prepared by RF reactive magnetron sputtering at different substrate temperatures and O_2 fluxes. *Journal of Alloys and Compounds*, *719*, pp.429–437.

23. Priyadarshini, D.M., Mannam, R., Rao, M.S.R. and DasGupta, N., **2017**. Effect of annealing ambient on SnO_2 thin film transistors. *Applied Surface Science*, *418*, pp.414–417.

24. Luo, H., Liang, L.Y., Cao, H.T., Dai, M.Z., Lu, Y.C. and Wang, M., **2015**. Control of ambipolar transport in SnO thin-film transistors by back-channel surface passivation for high performance complementary-like inverters. *ACS Applied Materials & Interfaces*, *7*(31), pp.17023–17031.

25. X-ray Photoelectron Spectroscopy (XPS) Reference Pages, (http://www.xpsfitting.com/search/label/Tin).

26. Hung, C.-H., Wang, S.-J., Liu, P.-Y., Wu, C.-H., Yan, H.-P., Wu, N.-S. and Lin, T.-H., **2017**. Improving the electrical and hysteresis performance of amorphous IGZO thin-film transistors using co-sputtered zirconium silicon oxide gate dielectrics. *Materials Science in Semiconductor Processing*, *67*, pp.84–91.

27. Xie, H., Xu, J., Liu, G., Zhang, L. and Dong, C., **2017**. Development and analysis of nitrogen-doped amorphous InGaZnO thin film transistors. *Materials Science in Semiconductor Processing*, *64*, pp.1–5.

28. Kim, M.-H., Choi, M.-J., Kimura, K., Kobayashi, H. and Choi, D.-K., **2016**. Improvement of the positive bias stability of a-IGZO TFTs by the HCN treatment. *Solid-State Electronics*, *126*, pp.87–91.

29. Joo, Y.-H. and Kim, C.-I., **2015**. High-density plasma etching characteristics of indium–gallium–zinc oxide thin films in CF_4/Ar plasma. *Thin Solid Films*, *583*, pp.40–45.

Received: 9 November 2018. Accepted: 26 March 2019.